Cooperative diagnostics for distributed LSDM systems based on triangulation

Cooperative diagnostics for distributed LSDM systems based on triangulation

Franceschini F. [1], Maisano D. [1], Mastrogiacomo L. [1]
[1] Politecnico di Torino (DIGEP), Torino, ITALY, domenico.maisano@polito.it.

Abstract

In the field of *large-scale dimensional metrology* (LSDM), new distributed systems based on different technologies have blossomed over the last decade. They generally include (i) some targets to be localized and (ii) a network of portable devices, distributed around the object to be measured, which is often bulky and difficult to handle.
The objective of this paper is to present some diagnostic tests for those distributed LSDM systems that perform the target localization by triangulation. Three are the tests presented: two *global* tests to detect the presence of potential anomalies in the system during measurements, and one *local* test aimed at isolating any faulty network device(s). This kind of diagnostics is based on the *cooperation* of different network devices that merge their local observations, not only for target localization, but also for detecting potential measurement anomalies.
Tests can be implemented in real-time, without interrupting or slowing down the measurement process.
After a detailed description of the tests, we present some practical applications on MSCMS-II, a distributed LSDM system based on infrared photogrammetric technology, recently developed at DIGEP-Politecnico di Torino.

Keywords: Large-scale dimensional metrology, Distributed measuring system, Triangulation, Model-based redundancy, Cooperative diagnostics, On-line diagnostics, Statistical test.

1. INTRODUCTION AND LITERATURE REVIEW

In the last decade there has been an increasing development of distributed dimensional metrology systems, i.e., instruments consisting of multiple devices that are positioned around the object to be measured and cooperate during the measurement activity [1, 2, 3]. The majority of these systems have been developed in the field of *large-scale dimensional metrology* (LSDM), concerning the measurement of medium to large-sized objects (i.e., according to the definition by Puttock [4], "*objects with linear dimensions ranging from tens to hundreds of meters*"), in industrial environments. Typical industrial applications are (i) reconstruction of curves/surfaces for dimensional verification and (ii) assembly of large-sized mechanical components, in which levels of accuracy of a few millimetres are generally tolerated.

The reason behind the development of distributed LSDM systems is simple: arranging a portable measuring instrument around the object to be measured is often more practical than the vice-versa [5].
Existing measuring systems differ in technology (e.g., laser optical, photogrammetric, interferometric, ultrasound, etc.); some of these are consolidated and available on the market, while others are only prototypes. Table 1 classifies some systems, reporting key features and bibliographic references for the reader.

Name	Technology	Current level of development	Localization technique	Bibliographic reference
Nikon iGPS	Laser-optical	Commercial	Triangulation	[6]
3rd Tech HiBall	Infrared, LED	Semi-commercial	Triangulation	[8]
Multiple Laser Trackers	Interferometric, ADM	Semi-commercial	Multilateration	[7]
MScMS-I	Ultrasound	Prototype	Multilateration	[1]
MScMS-II	Infrared photogrammetric	Prototype	Triangulation	[9]

Table 1. Classification of some of the existing distributed LSDM systems.

The common features of these systems are (see Figure 1):

1. a *network of devices* distributed around the object to be measured;
2. a *hand-held probe* for measuring the spatial Cartesian coordinates (*XYZ*) of the points of interest;
3. a centralized *data processing unit* (DPU), which receives local measurement data from network devices.

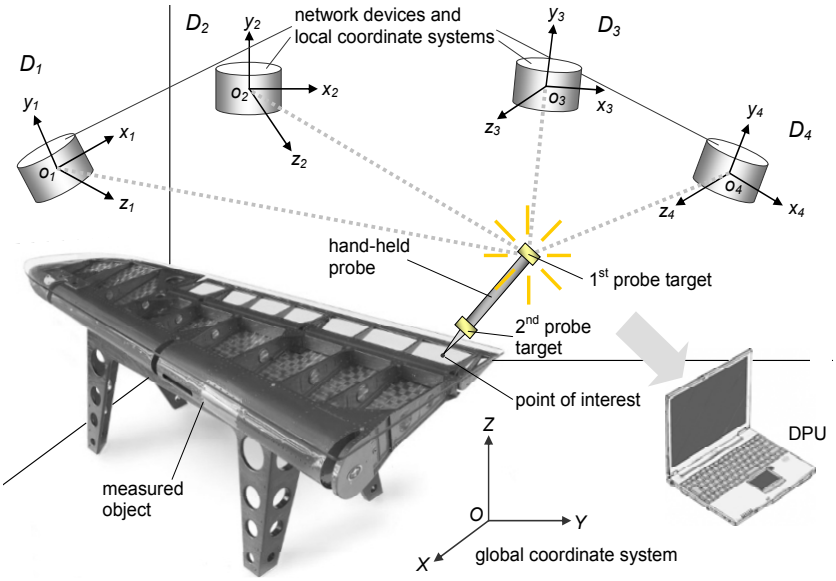

Figure 1. Schematic representation of a generic distributed LSDM system.

The probe is equipped with some targets (at least two) that, after being localized, allow to determine the probe position/orientation and – consequently – the position of the point of interest, generally in contact with a tip. In certain cases (e.g., for MScMS-II) probe targets are passive sensors, while in others (e.g., for iGPS) they are active and can have a processing capability which makes them able to perform local measurements (typically angles or distances) with respect to each network device.
As shown in Table 1, there are two typical techniques for localizing probe targets [10]:

- *Triangulation*, using the angles subtended by the targets, from the local perspective of (at least two) network devices;
- *Multilateration*, using the distances between the targets and (at least three) network devices.

The number of devices involved in the localization of a target depends on their mutual positioning/orientation and communication range.
For distributed LSDM systems, as well as for metrological systems in general, reliability of measurements is essential and can be increased by the use of real time diagnostic tools able to detect measurement accidents and discard/correct (part of) the measurement results.
The purpose of this article is to present some novel statistical tests for the on-line diagnostics of distributed LSDM systems based on triangulation, in the case of quasi-static measurements – i.e., targets are stationary or are moved at very low speeds during their localization. These tests make it possible to identify possible measurement accidents and, subsequently, to isolate the (potentially) faulty network devices. This kind of diagnostics can be classified as *cooperative*, since it is based on the cooperation of different network devices that merge their local angular measurements.
The three statistical tests that will be discussed are divided in two categories:

- Two *global tests* aimed at evaluating the reliability of measurements, based on their variability.
- A *local test* that – when a measurement is not considered reliable by (at least one of) the global tests – identifies the potentially faulty device(s) and (temporarily) excludes them from the measurement process, without interrupting it.

After a detailed description of each test, we will show some real application examples using MScMS-II, a prototypical distributed LSDM system based on infrared photogrammetric technology, recently developed at the Industrial Metrology and Quality Engineering Laboratory of DIGEP – Politecnico di Torino.
The remaining of this paper is structured in four sections. Section 2 provides some background information, which is helpful to grasp the subsequent description of statistical tests: (i) basic concepts concerning distributed LSDM systems' diagnostics, (ii) a general description of the localization problem for systems based on triangulation, and (iii) a brief description of MScMS-II, on which the diagnostic tests will be implemented. Section 3 provides a detailed description of the statistical tests (global and local respectively) with some experimental examples. Finally, Section 4

summarizes the original contributions of this research, focusing on its implications, limitations and possible future developments.

2. BACKGROUND INFORMATION

2.1 Basic concepts concerning diagnostics

In general, the concept of *reliability* (or *consistency*) *of a measurement* is defined as follows. For each measurable quantity *x*, we can define an acceptance interval [*LAL*, *UAL*] (where *LAL* stands for Lower Acceptance Limit and *UAL* for Upper Acceptance Limit) [1]. The measure x_M of the quantity *x*, produced by a measurement system, is considered reliable if $x_M \in [LAL, UAL]$.

The type-I and -II probability errors (misclassification rates) respectively correspond to:

$$\begin{aligned} \alpha &= \Pr\{x_M \notin [LAL, UAL] \mid \text{absence of systematic meaurement error sources}\} \\ \beta &= \Pr\{x_M \in [LAL, UAL] \mid \text{presence of systematic meaurement error sources}\}. \end{aligned} \quad (1)$$

Usually, *LAL* and *UAL* are defined considering the natural variability of the measuring system (which is linked to its metrological characteristics of accuracy, reproducibility, repeatability, etc.), in the absence of systematic error sources[1] [11].

Note that the above definitions of reliability, acceptance interval, type-I and -II error refer to the result of a specific measurement and not to the overall metrological performance of a measuring system.

For distributed systems, local anomalies of one or more network devices can distort or even compromise the whole measurement. On the other hand, when these anomalies are recognised, the measurement results can be corrected, (temporarily) excluding malfunctioning device(s). This is the reason why distributed systems are – to some extent – rather "vulnerable", but can be successfully protected by appropriate diagnostic tools.

For distributed systems, a typical diagnostic approach is based on the so-called *model-based redundancy*, where the replication of a physical instrumentation – which is typical of the *physical redundancy* approach – is substituted by the use of appropriate mathematical models [12]. These models may derive from physical laws applied to experimental data or from self-learning method (for example, neural networks) and allow the detection of system failures by comparing measured and model-elaborated process variables. This diagnostic approach is made possible by the fact that, for distributed systems, the number of network devices generally involved in a measurement is greater than the number strictly necessary for performing the localization of target(s).

---

[1] The authors are aware that systematic errors can never be eradicated completely. The assumption of random errors only is therefore not valid in general, even though could be adequate for the purpose of diagnostics.

This type of diagnostics is based on the *cooperation* of network devices, whose local observations are used in conjunction, not only for target localization, but also for detecting possible measurement anomalies or accidents.
Diagnostic tools based on this philosophy are implemented for GPS-assisted aircraft navigation, where the GPS can be seen as a very-large-scale dimensional metrology distributed system, in which localization is performed by multilateration [13]. Furthermore, Franceschini et al. [14] give a detailed description of some on-line diagnostic tools for MScMS-I, an indoor distributed LSDM system based on multilateration.
As mentioned in Sect. 1, this diagnostics generally includes two types of tests (global and local), aimed respectively at (i) evaluating unreliable measurements and (ii) identifying and (temporarily) excluding purportedly faulty network devices. The flowchart in Figure 2 illustrates a typical sequence of implementation of these tests.

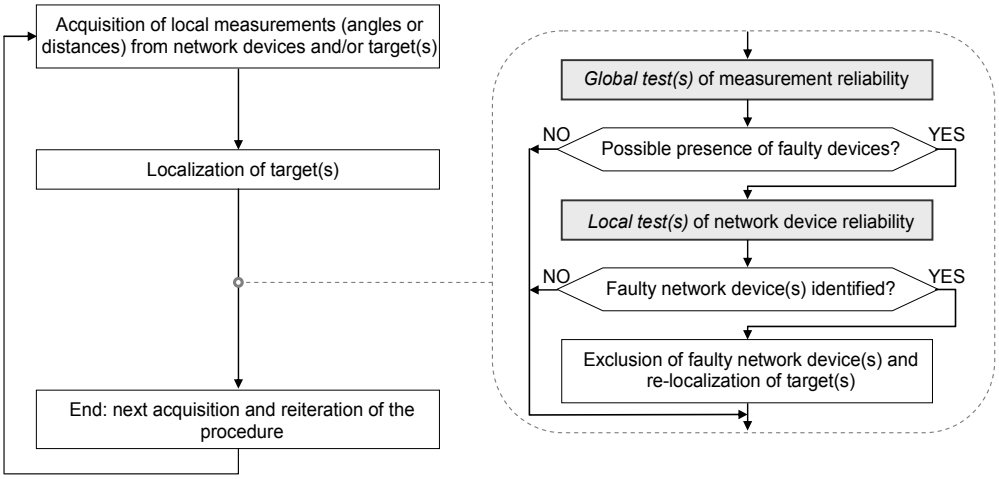

(a) localization procedure (b) on-line system diagnostics

Figure 2. Flowchart showing the logical implementation sequence relating to the on-line diagnostic tests.

2.2 The triangulation problem

Figure 1 depicts a distributed LSDM system consisting of a number of network devices ($D_1 \ldots D_N$) positioned around the object to be measured. *OXYZ* is a global Cartesian coordinate system. Each of the devices has its own spatial position and orientation; for each *i*-th device, it is defined a local coordinate system $o_i x_i y_i z_i$, roto-translated with respect to *OXYZ*.
A general transformation between a local and the global coordinate system is given by:

$$\boldsymbol{X} = \boldsymbol{R_i}\,\boldsymbol{x_i} + \boldsymbol{X_{0_i}} \Rightarrow \begin{bmatrix} X \\ Y \\ Z \end{bmatrix} = \begin{bmatrix} r_{11_i} & r_{12_i} & r_{13_i} \\ r_{21_i} & r_{22_i} & r_{23_i} \\ r_{31_i} & r_{32_i} & r_{33_i} \end{bmatrix} \begin{bmatrix} x_i \\ y_i \\ z_i \end{bmatrix} + \begin{bmatrix} X_{0_i} \\ Y_{0_i} \\ Z_{0_i} \end{bmatrix}. \quad (2)$$

$\boldsymbol{R_i}$ is a rotation matrix, which elements are functions of three rotation parameters (see Figure 3):

$$\boldsymbol{R_i} = \begin{bmatrix} \cos\phi_i \cos\kappa_i & -\cos\phi_i \sin\kappa_i & \sin\phi_i \\ \cos\omega_i \sin\kappa_i + \sin\omega_i \sin\phi_i \cos\kappa_i & \cos\omega_i \cos\kappa_i - \sin\omega_i \sin\phi_i \sin\kappa_i & -\sin\omega_i \cos\phi_i \\ \sin\omega_i \sin\kappa_i - \cos\omega_i \sin\phi_i \cos\kappa_i & \sin\omega_i \cos\kappa_i + \cos\omega_i \sin\phi_i \sin\kappa_i & \cos\omega_i \cos\phi_i \end{bmatrix}, \quad (3)$$

where:

ω_i represents a counterclockwise rotation around the x_i axis;

ϕ_i represents a counterclockwise rotation around the new y_i axis (i.e., y_i'), which was rotated by ω_i;

κ_i represents a counterclockwise rotation around the new z_i axis (i.e., z_i''), which was rotated by ω_i and then ϕ_i.

$\boldsymbol{X_{0_i}} = \left[X_{0_i}, Y_{0_i}, Z_{0_i}\right]^T$ are the coordinates of the origin of $o_i x_i y_i z_i$, in the global coordinate system *OXYZ*.

The (six) location/orientation parameters related to each network device (i.e., $X_{0_i}, Y_{0_i}, Z_{0_i}$, ω_i, ϕ_i, κ_i) are treated as known parameters, since they are measured in an initial calibration process [15].

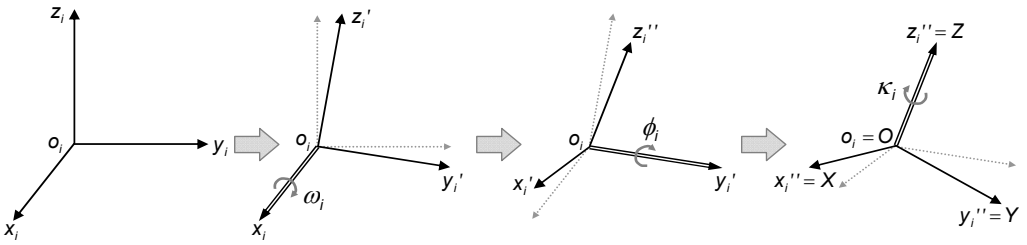

Figure 3. Rotation parameters regarding the transformation between a local coordinate system ($o_i x_i y_i z_i$) and the global one (*OXYZ)*.

The point to be located is $P \equiv (X, Y, Z)$. From the local perspective of each *i*-th device, two angles – i.e., θ_{c_i} (azimuth) and φ_{c_i} (elevation) – are subtended by the line passing through *P* and a local *observation point*, which we assume as coincident with the origin $o_i \equiv (0, 0, 0)$ of the local coordinate system (see Figure 4). Precisely, φ_{c_i} describes the inclination of segment $o_i P$ with respect to the plane $x_i y_i$ (with a positive

sign when z_i>0), while θ_{c_i} describes the counterclockwise rotation of the projection (o_iP') of o_iP on the x_iy_i plane, with respect to the x_i axis. For each *i*-th local coordinate system, the two angles are given respectively by:

$$\theta_{c_i} = \tan^{-1}\frac{y_i}{x_i} \qquad \begin{cases} \text{if } x_i \geq 0 \text{ then } -\frac{\pi}{2} \leq \theta_{c_i} \leq \frac{\pi}{2} \\ \text{if } x_i < 0 \text{ then } \frac{\pi}{2} < \theta_{c_i} < \frac{3\pi}{2} \end{cases}. \tag{4}$$

$$\varphi_{c_i} = \tan^{-1}\frac{z_i}{\sqrt{x_i^{\,2} + y_i^{\,2}}} \qquad \left\{ -\frac{\pi}{2} \leq \varphi_{c_i} \leq \frac{\pi}{2} \right.$$

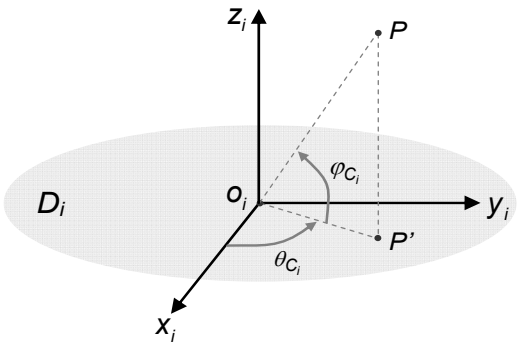

Figure 4. For a generic network device (D_i), two angles – i.e., θ_{c_i} (azimuth) and φ_{c_i} (elevation) – are subtended by a line joining the point *P* (to be localized) and the origin o_i of the local coordinate system $o_ix_iy_iz_i$.

Regarding the two angles in Eq. 4, the subscript "c_i" means that – for the *i*-th network device – they are *calculated* as functions of the local coordinates of $P \equiv (x_i, y_i, z_i)$. θ_{c_i} and φ_{c_i} can be expressed as functions of the global coordinates of point *P*. Eq. 5 is the reverse formula for switching from a local coordinate system to the global; since $\boldsymbol{R}$ is orthonormal, then $\boldsymbol{R_i^{-1}} = \boldsymbol{R_i^T}$ [15].

$$\boldsymbol{x_i} = \boldsymbol{R}_i^{-1}\left(\boldsymbol{X} - \boldsymbol{X_{0_i}}\right) = \boldsymbol{R}_i^{T}\left(\boldsymbol{X} - \boldsymbol{X_{0_i}}\right) \Rightarrow$$

$$\begin{cases} x_i = r_{11_i}\left(X - X_{0_i}\right) + r_{21_i}\left(Y - Y_{0_i}\right) + r_{31_i}\left(Z - Z_{0_i}\right) \\ y_i = r_{12_i}\left(X - X_{0_i}\right) + r_{22_i}\left(Y - Y_{0_i}\right) + r_{32_i}\left(Z - Z_{0_i}\right) \\ z_i = r_{13_i}\left(X - X_{0_i}\right) + r_{23_i}\left(Y - Y_{0_i}\right) + r_{33_i}\left(Z - Z_{0_i}\right) \end{cases}. \tag{5}$$

The resulting formulae of θ_{c_i} and φ_{c_i} are obtained combining Eqs. 4 and 5:

$$\theta_{C_i}(X,Y,Z) = \tan^{-1}\frac{r_{12_i}(X-X_{0_i})+r_{22_i}(Y-Y_{0_i})+r_{32_i}(Z-Z_{0_i})}{r_{11_i}(X-X_{0_i})+r_{21_i}(Y-Y_{0_i})+r_{31_i}(Z-Z_{0_i})}$$
$$\varphi_{C_i}(X,Y,Z) = \tan^{-1}\frac{r_{13_i}(X-X_{0_i})+r_{23_i}(Y-Y_{0_i})+r_{33_i}(Z-Z_{0_i})}{o_iP'}, \quad (6)$$

being:

$$o_iP' = \sqrt{\left(r_{11_i}(X-X_{0_i})+r_{21_i}(Y-Y_{0_i})+r_{31_i}(Z-Z_{0_i})\right)^2+\left(r_{12_i}(X-X_{0_i})+r_{22_i}(Y-Y_{0_i})+r_{32_i}(Z-Z_{0_i})\right)^2} \quad (7)$$

Using the two angular local measurements (θ_{M_i} and φ_{M_i}) performed by each *i*-th network device, one can set up a system of equations for calculating the three unknown coordinates of *P*, as:

$$\begin{cases}\begin{cases}\theta_{M_1}=\theta_{C_1}(X,Y,Z)\\ \varphi_{M_1}=\varphi_{C_1}(X,Y,Z)\end{cases}\\ \begin{cases}\theta_{M_2}=\theta_{C_2}(X,Y,Z)\\ \varphi_{M_2}=\varphi_{C_2}(X,Y,Z)\end{cases}\\ \ldots\\ \begin{cases}\theta_{M_N}=\theta_{C_N}(X,Y,Z)\\ \varphi_{M_N}=\varphi_{C_N}(X,Y,Z)\end{cases}\end{cases}, \quad (8)$$

where *N* is the number of network devices (with *a priori* known location and orientation) involved in the measurement.

The system in Eq. 8 can be solved when *P* is "seen" by at least two devices (2 angles x 2 devices = 4 total equations). Since the triangulation problem is overdefined (more equations than unknown parameters), it can be solved using a minimization approach [16]. The position of *P* can be estimated by the iterative minimization of a suitable Error Function *EF*. A simple option can be given by:

$$EF(P) = \frac{1}{N}\left\{\sum_{i=1}^{N}\left[\left(\theta_{M_i}-\theta_{C_i}\right)^2/\sigma_{\theta_i}^2\right]+\sum_{i=1}^{N}\left[\left(\varphi_{M_i}-\varphi_{C_i}\right)^2/\sigma_{\varphi_i}^2\right]\right\}, \quad (9)$$

where:

P is the point to be localized, whose unknown coordinates (*X*, *Y*, *Z*) are the solution of the problem.

θ_{M_i} and φ_{M_i} are the angles locally measured by each *i*-th device (input data of the problem).

θ_{C_i} and φ_{C_i} are the angles calculated for each *i*-th device (Eq. 6), using the coordinates (*X*, *Y*, *Z*) resulting from the solution of the system. This solution is iterative: each iteration leads to determining an attempt solution, gradually converging to the point of global minimum of the *EF*.

$\sigma^2_{\theta_i}$ and $\sigma^2_{\varphi_i}$ are the (supposed known) variances related to the difference between measured and calculated angles, i.e., defined as residuals $\left(\theta_{M_i} - \theta_{C_i}\right)$ and $\left(\varphi_{M_i} - \varphi_{C_i}\right)$. Since these residuals may have different dispersion, they are weighted by the reciprocal of their variance [17].

N is the number of network devices involved in the measurement.

We remark that the determination of the θ_{M_i} and φ_{M_i} values depends on the specific technology of the measuring instrument. For example, in the case of the iGPS, they are determined by the target, measuring the period between the detection of two laser blades emitted by each *i*-th network device [6]. Besides, for systems based on photogrammetry, such as MScMS-II, they are obtained on the basis of the position of the target in a local image related to the *i*-th network device [9].

Also, there are many possible choices of the *EF* to minimize for solving the localization problem. We defined that one in Eq. 9 trying to keep it as simple and general as possible. A more sophisticated (but also complex) option would be to weigh the angular residuals by the reciprocal of the distances between target and network devices of interest, according to an iterative procedure. This option would reflect the fact that – for a certain angular deviation – the target position error tends to increase proportionally with distances from network devices.

Since the proposed *EF* is non-linear, its minimization can be computationally expensive. The burden of computation can be eased by employing a suitable linearization technique.

2.3 The MScMS-II

The MScMS-II (i.e., Mobile Spatial coordinate Measuring System-II) is a prototypical measuring instrument, based on infrared (IR) photogrammetric technology. Network devices are low-cost IR cameras associated with IR illuminators, while the hand-held probe has two reflective spheres, whose centres are *A* and *B*, and a tip (*V*), in contact with the point(s) of interest (see Figure 5). The reflective spheres are passive targets illuminated by the illuminators. Alternatively, one can use active spherical targets that emit IR light, not making it necessary to use illuminators.

The localization of the probe targets allows to uniquely determine the coordinates of the probe tip, being *A*, *B* and *V* positioned on the same line, at known distances [9].

We now focus the attention on each *i*-th network device (camera). Given the position $P'' \equiv (u_i, v_i)$ of the projection of target *P* on the camera's image plane $u_i v_i$ – which is parallel to the plane $x_i y_i$ of the local coordinate system – and knowing some internal parameters of the camera – i.e., the focal length (f_i) – it is possible to determine the angles θ_{M_i} and φ_{M_i} (see Figure 6):

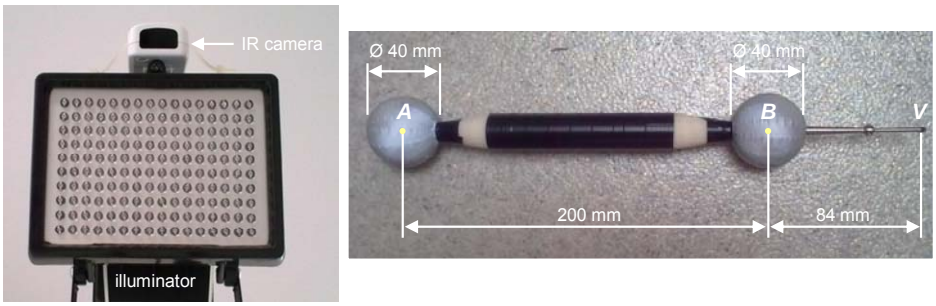

(a) (b)

Figure 5. Elementary components of the MScMS-II: (a) IR cameras and illuminators, and (b) hand-held probe with two spherical targets (*A* and *B*) and a tip (*V*).

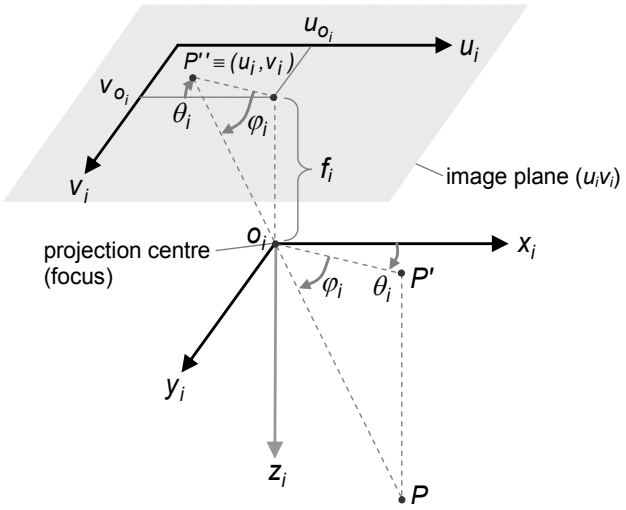

Figure 6. For a generic *i*-th network device, representation of the local coordinate system, with origin (o_i) in the projection centre (or focus), and the image plane $u_i v_i$ – parallel to the plane $x_i y_i$, at a distance f_i (i.e., the focal length).

$$\theta_{M_i} = \tan^{-1}\frac{v_i - v_{0_i}}{u_i - u_{0_i}} \qquad \begin{cases} \text{if } u_i - u_{0_i} > 0 \text{ then } \dfrac{\pi}{2} < \theta_{M_i} < \dfrac{3\pi}{2} \\ \text{if } u_i - u_{0_i} \le 0 \text{ then } -\dfrac{\pi}{2} \le \theta_{M_i} \le \dfrac{\pi}{2}, \end{cases} \qquad (10)$$

$$\varphi_{M_i} = \tan^{-1}\frac{f_i}{\sqrt{\left(u_i - u_{0_i}\right)^2 + \left(v_i - v_{0_i}\right)^2}} \qquad \left\{ -\frac{\pi}{2} \le \varphi_{M_i} \le \frac{\pi}{2} \right.$$

where:

u_i and v_i are the coordinates of the projection (P'') of P on the image plane;

u_{0_i} and v_{0_i} are the coordinates of the projection of o_i on the plane $u_i v_i$;

f_i is the distance between the plane $u_i v_i$ and the camera projection centre (or focus), which is coincident with the origin o_i of the local coordinate system $o_i x_i y_i z_i$.

We note that θ_{M_i} and φ_{M_i} are not measured directly: the "primary" quantities, i.e., those measured directly by each i-th network device, are the coordinates of $P'' \equiv (u_i, v_i)$. The angles of interest can be then obtained through the formulae in Eq. 10. Of course, for systems based on other technologies, primary measured quantities may be different.

Angles θ_{M_i} and φ_{M_i} can be compared with θ_{C_i} and φ_{C_i}, i.e., those calculated as functions of the (unknowns) coordinates of P (Eq. 6), so as to solve the localization problem by the *EF* minimization (in Eq. 9).

Being based upon IR optical technology, MScMS-II is sensible to many influencing factors. The most common measurement accidents are:

- Vibration or accidental movement of the cameras;
- Partial occlusion (e.g., by obstacles interposed between network device(s) and target(s)) or target overlapping;
- False targets due to IR light reflection on polished surfaces or the presence of other external uncontrolled IR light sources.

These and other potential causes of accidental measurement errors must be taken under control to assure an acceptable level of accuracy.

3. ON-LINE DIAGNOSTIC TESTS

With the aim of protecting the system, MScMS-II implements some statistical tests for on-line diagnostics. Three tests are analysed in the following sub-sections:

1. Test 1: Global test on the *EF*;
2. Test 2: Global test on the distance between probe targets;
3. Test 3: Local test for identifying purportedly faulty device(s).

3.1 Test 1: Global test on the *EF*

By definition (see Eq. 9), $EF(P) \geq 0$ for all the points in the measurement volume $\xi \subseteq \Re^3$. In particular, $EF(P) = 0$ when $\theta_{M_i} = \theta_{C_i}$ and $\varphi_{M_i} = \varphi_{C_i}$, for $i = 1 \ldots N$.

Because of the measurement natural variability, two situations may occur:

- $EF(P)$ is strictly positive even in the point of correct localization;
- $EF(P)$ converges to a point that is not the correct one. As a result, a local minimum may be confused with the global minimum.

The first diagnostic criterion is aimed at identifying all the non-acceptable minima solutions for *EF*(*P*), in order to prevent system fails. Such criterion enables MScMS-II to distinguish between reliable and unreliable measurements.
Let consider a solution $P \equiv (X, Y, Z)$ to the problem $\min_{P \in \xi} EF(P)$. In general, being the problem overdetermined (as shown in Eq. 8) and since single measurements are affected by noise, a solution that exactly satisfies all angular constrains is not realistically possible. In real conditions, there are two types of residuals: $\varepsilon_{\theta_i} = (\theta_{M_i} - \theta_{C_i})$ and $\varepsilon_{\varphi_i} = (\varphi_{M_i} - \varphi_{C_i})$. In absence of systematic error causes, it is reasonable to hypothesize that they follow two zero-mean normal distributions, i.e. $\varepsilon_{\theta_i} \sim N(\mu_\theta \approx 0, \sigma_{\theta_i}^2)$ and $\varepsilon_{\varphi_i} \sim N(\mu_\varphi \approx 0, \sigma_{\varphi_i}^2)$. These assumptions will be tested empirically.
If $\sigma_{\theta_i} = \sigma_\theta$ and $\sigma_{\varphi_i} = \sigma_\varphi$, $\forall i$ (this is true in absence of spatial/directional effects), Eq. 9 becomes:

$$EF(P) = \frac{1}{N} \cdot \left(\sum_{i=1}^{N} \frac{\varepsilon_{\theta_i}^2}{\sigma_\theta^2} + \sum_{i=1}^{N} \frac{\varepsilon_{\varphi_i}^2}{\sigma_\varphi^2} \right) = \frac{1}{N} \cdot \left(\sum_{i=1}^{N} z_{\theta_i}^2 + \sum_{i=1}^{N} z_{\varphi_i}^2 \right). \tag{11}$$

EF(*P*) can be seen as the sum of the squares of *N* + *N* realizations of two series of normally distributed random variables (z_{θ_i} and z_{φ_i}) with mean 0 and variance 1, multiplied by the constant term 1/*N*.
Eq. 11 therefore can assume the following form:

$$EF(P) = \frac{1}{N} \cdot \left(\chi_\theta^2 + \chi_\varphi^2 \right), \tag{12}$$

where:

χ_θ^2 and χ_φ^2 are two chi-square distributed random variables, with *N* degrees of freedom (DOF) each, since they are obtained by the sum of *N* independent terms;
N is the number of network devices involved in the measurement.

The residual standard deviations, i.e., σ_θ and σ_φ, can be *a priori* estimated for the whole measurement volume, for example during the phase of installation and calibration of the system.
Eq. 12 can be expressed as:

$$EF(P) = \frac{1}{N} \cdot \chi^2, \tag{13}$$

Since χ^2 is obtained by adding two chi-square distributed variables with *N* DOF each, it will follow a chi-square distribution with 2·*N* DOF [17].
Every time the localization of a probe target is performed, MScMS-II diagnostics calculates the following quantity:

$$\chi^2 = EF(P) \cdot N. \tag{14}$$

Assuming a risk α as a type-I error, a one-sided confidence interval for the variable χ^2 can be calculated. $\chi^2_{\nu,1-\alpha}$ is a chi-square distribution with $\nu = 2 \cdot N$ DOF and a $(1-\alpha)$ confidence coefficient. The confidence interval is assumed as the acceptance interval for the reliability test of the measurement.
The test drives to the following two alternative conclusions:

$EF = \chi^2 / N \leq \chi^2_{\nu,1-\alpha} / N \rightarrow$ measurement is considered reliable;

$EF = \chi^2 / N > \chi^2_{\nu,1-\alpha} / N \rightarrow$ measurement is considered unreliable, hence it is rejected.

3.1.1 Set up of test parameters

The risk level α is established by the user. A high α prevents from non-acceptable solutions of the minimization problem, although it might drive to reject good solutions.
On the other hand, a low α speeds up the measurement procedure, although it might drive to collect wrong data due to the consequent increase of the type-II error β.
The residual standard deviations σ_θ and σ_φ can be determined empirically, on the basis of experimental angle measurements. In this case, σ_θ and σ_φ are estimated from the residuals obtained by measuring a sample of points randomly distributed in the whole measurement volume $\xi \subseteq \Re^3$, in the absence of systematic error sources. This operation can be implemented during the initial phase of system set-up and calibration.
Given a set of M points randomly distributed in the measurement volume and measured by a single target (with a random sequence of measurements), two sets of N_j residuals (i.e., $\varepsilon_{\theta_{ij}}$ and $\varepsilon_{\varphi_{ij}}$) can be calculated for each j-th point ($j = 1 \ldots M$, $i = 1 \ldots N_j$). The number N_j may change due to the number of network devices involved in each measurement.
In absence of systematic error causes and time or spatial/directional effects, it is reasonable to hypothesize that $\varepsilon_{\theta_{ij}}$ and $\varepsilon_{\varphi_{ij}}$ are zero-mean normally distributed random variables, i.e.:

$$\varepsilon_{\theta_{ij}} = \left(\theta_{M_i} - \theta_{C_i}\right)_j \sim N\left(\mu_\theta \approx 0, \sigma_\theta^2\right) \text{ and } \varepsilon_{\varphi_{ij}} = \left(\varphi_{M_i} - \varphi_{C_i}\right)_j \sim N\left(\mu_\varphi \approx 0, \sigma_\varphi^2\right), \quad (15)$$

being $\hat{\mu}_\theta = \left(\sum_{j=1}^{M}\sum_{i=1}^{N_j} \varepsilon_{\theta_{ij}}\right) \Big/ \left(\sum_{j=1}^{M} N_j\right) \approx 0$ and $\hat{\mu}_\varphi = \left(\sum_{j=1}^{M}\sum_{i=1}^{N_j} \varepsilon_{\varphi_{ij}}\right) \Big/ \left(\sum_{j=1}^{M} N_j\right) \approx 0$ (to be tested).
The standard deviations σ_θ and σ_φ may be estimated as follows:

$$\hat{\sigma}_\theta = \sqrt{\left[\sum_{j=1}^{M}\sum_{i=1}^{N_j}\left(\varepsilon_{\theta_{ij}} - \hat{\mu}_\theta\right)^2\right] \Big/ \left[\left(\sum_{j=1}^{M} N_j\right) - 1\right]}$$
$$\hat{\sigma}_\varphi = \sqrt{\left[\sum_{j=1}^{M}\sum_{i=1}^{N_j}\left(\varepsilon_{\varphi_{ij}} - \hat{\mu}_\varphi\right)^2\right] \Big/ \left[\left(\sum_{j=1}^{M} N_j\right) - 1\right]}. \quad (16)$$

The resulting values of $\hat{\sigma}_\theta$ and $\hat{\sigma}_\varphi$ are used as reference values for the test. With this notation, Eq. 13 becomes:

$$\chi^2 = EF(P) \cdot N \approx \sum_{i=1}^{N} \frac{\varepsilon_{\theta_i}^2}{\hat{\sigma}_\theta^2} + \sum_{i=1}^{N} \frac{\varepsilon_{\varphi_i}^2}{\hat{\sigma}_\varphi^2}. \quad (17)$$

3.1.2 Experimental example

It was used a network consisting of six cameras ($D_1 \ldots D_6$) with known position and orientation, distributed in the measurement volume as schematized in Figure 7. The standard deviations σ_θ and σ_φ were empirically estimated according to the following steps:

- M = 290 points, randomly distributed in the measurement volume, were measured using a single target.
- The coordinates of each point (P_j, j = 1…M) were evaluated by minimizing the *EF* in Eq. 9. As regards $\varepsilon_{\theta_{ij}}$ and $\varepsilon_{\varphi_{ij}}$, two sets of 1740 residuals each were obtained.
- Measurements were performed in a controlled environment (e.g., temperature, light and vibrations were kept under control) and the distributions of residuals were thoroughly analyzed, in order to exclude measurement accidents, e.g., time or spatial/directional effects, or non-random causes of variation in general.
- The zero-mean normal distribution of each of the two sets of residuals was verified by the Anderson-Darling normality test at $p<0.05$ [17].
- The standard deviations of the two sets of residuals were estimated by Eq. 16. Table 2 reports the resulting $\hat{\sigma}_\theta$ and $\hat{\sigma}_\varphi$ values and other data concerning them.

We remark that (i) the mean value of both the sets of residuals is roughly zero and (ii) the $\hat{\sigma}_\theta$ value is one order of magnitude higher than the $\hat{\sigma}_\varphi$. The latter behaviour is due to geometric reasons concerning the determination of θ_{M_i} and φ_{M_i}, using the coordinates (u_i, v_i) of the target on one camera's local image plane (see Eq. 10).
The hypothesis that $\varepsilon_{\theta_{ij}}$ and $\varepsilon_{\varphi_{ij}}$ values have the same standard deviations (σ_θ and σ_φ) $\forall\, j$ = 1…M, i = 1…N_j as well as the σ_θ and σ_φ estimates may be undermined by particularities regarding the layout of network devices. However, we observed that,

when devices are uniformly distributed around the measurement volume, results are not significantly dissimilar, even for different network layouts.

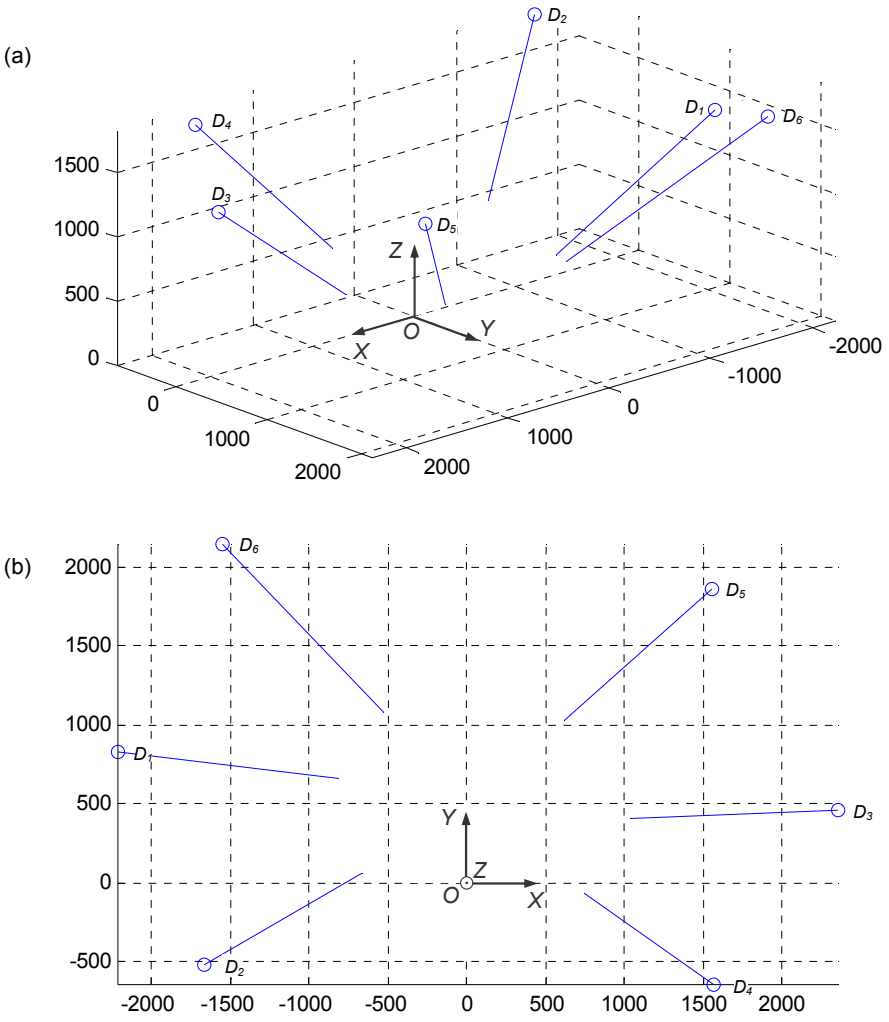

Figure 7. Representation of the positioning and orientation of the MScMS-II network devices used in the application example: (a) 3D view and (b) *XY* plane view. *OXYZ* is the global coordinate system (coordinates in millimetres). The measuring volume contains six network cameras ($D_1 \ldots D_6$), whose outgoing vectors (in blue) represent their orientation.

Sample size: $N_{TOT} = \sum_{j=1}^{M} N_j$	N_{TOT} = 1740
Mean value estimates: $\hat{\mu}_\theta = \left(\sum_{j=1}^{M} \sum_{i=1}^{N_j} \varepsilon_{\theta_{ij}} \right) \Big/ \left(\sum_{j=1}^{M} N_j \right)$ and $\hat{\mu}_\varphi = \left(\sum_{j=1}^{M} \sum_{i=1}^{N_j} \varepsilon_{\varphi_{ij}} \right) \Big/ \left(\sum_{j=1}^{M} N_j \right)$	$\hat{\mu}_\theta$ = 0.301 $\hat{\mu}_\varphi$ = 0.004
Standard deviation estimates: $\hat{\sigma}_\theta = \sqrt{\left(\sum_{j=1}^{M} \sum_{i=1}^{N_j} \varepsilon_{\theta_{ij}}^2 \right) \Big/ \left(\sum_{j=1}^{M} N_j - 1 \right)}$ and $\hat{\sigma}_\varphi = \sqrt{\left(\sum_{j=1}^{M} \sum_{i=1}^{N_j} \varepsilon_{\varphi_{ij}}^2 \right) \Big/ \left(\sum_{j=1}^{M} N_j - 1 \right)}$	$\hat{\sigma}_\theta$ = 0.87 $\hat{\sigma}_\varphi$ = 0.06
Maximum: $\varepsilon_{\theta_{MAX}} = Max\{\varepsilon_{\theta ij} \mid i = 1...N_j, j = 1...M\}$ and $\varepsilon_{\varphi_{MAX}} = Max\{\varepsilon_{\varphi ij} \mid i = 1...N_j, j = 1...M\}$	$\varepsilon_{\theta_{MAX}}$ = 8.30 $\varepsilon_{\varphi_{MAX}}$ = 0.28
Minimum: $\varepsilon_{\theta_{MIN}} = Min\{\varepsilon_{\theta ij} \mid i = 1...N_j, j = 1...M\}$ and $\varepsilon_{\varphi_{MIN}} = Min\{\varepsilon_{\varphi ij} \mid i = 1...N_j, j = 1...M\}$	$\varepsilon_{\theta_{MIN}}$ = -11.60 $\varepsilon_{\varphi_{MIN}}$ = 0.29

Table 2. Detailed data concerning the estimation of σ_θ and σ_φ (angles in degrees).

In conditions of maximum visibility (i.e. *N*=6 network devices), the acceptance limit for *EF*, assuming a type-I risk level α = 0.05 and ν = 2·*N* = 2·6 = 12 DOF, becomes:

$$EF(P) \leq \frac{\chi^2_{\nu=12,1-\alpha=0.95}}{N} \Rightarrow EF(P) \leq \frac{21.0}{6} = 3.50 \,. \tag{18}$$

Let now consider a possible accident that can occur using a MScMS-II or a generic system based on IR photogrammetric technology for locating targets: *false targets*. Referring to the configuration in Figure 7, suppose that a generic point *P* inside the measurement volume has to be localized. All the network devices, with the exception of one, i.e., D_4, are able to correctly measure the angles (θ_{M_i} and φ_{M_i}) subtended by *P*. An obstacle, for example an operator who performs the measurement, is interposed between *P* and D_4, blocking it. At the same time, the IR light reflection on a polished surface within the measurement volume produces a false target (*F*). This false target is ignored by almost all devices, thanks to a selective technique according to which – in the presence of multiple targets – only those with greater light intensity (*P* in this case) are regarded as authentic, while others are excluded.

On the contrary, being unable to see *P* since it is blocked, device D_4 wrongly considers *F* as a target (see the representation in Figure 8). The consequence is that the angular measurements by D_4 are wrong. See the example in Table 3(a).

In this case, the algorithm will produce the following wrong localization solution: $P \equiv$ (104.0, 1062.2, 271.8) [mm], characterized by a high level of error:

$EF(P) \cong 28.02 > 3.50$. Owing to this result, this diagnostics suggests rejecting the measurement.

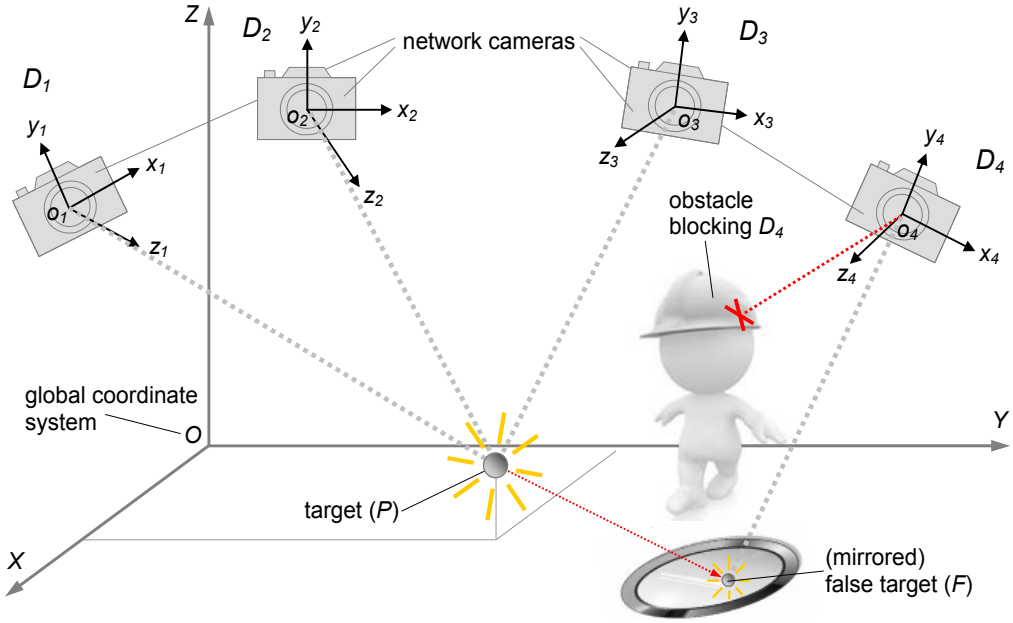

Figure 8. Representation of a possible measurement accident for the MScMS-II: the authentic target *P* (with high light intensity) is not detected by D_4, because of the interposed obstacle. On the other hand, the false target *F* – which is ignored by the other cameras because of the low light intensity – is erroneously detected by D_4.

Network device	(a) Measured angles		(b) Measured angles	
	θ_{M_i}	φ_{M_i}	θ'_{M_i}	φ'_{M_i}
D_1	28.16	77.16	28.25	77.14
D_2	214.39	76.95	214.39	76.95
D_3	142.70	73.34	142.72	73.36
D_4	(wrong) 311.78	(wrong) 72.65	(correct) 304.44	(correct) 72.96
D_5	352.49	79.86	352.49	79.86
D_6	185.16	80.08	185.16	80.08

Table 3. Example of angles measured by the MScMS-II network devices: (a) before and (b) after removing the cause of the measurement accident. Angles are expressed in degrees.

After removing the obstacle, the new angles observed by D_4 are θ'_{M_1} = 304.44 and φ'_{M_1} = 72.96 [degrees] while those relating to the remaining devices are almost identical to the previous ones (see Table 3(b)). The new localization is: $P \equiv$ (85.5, 1035.8, 299.6) [mm]. The corresponding *EF* value is $EF(P) \cong 2.13 \leq 3.50$. Hence, the new localization can be considered reliable and the measurement is accepted.

3.2 Test 2: Global test on the distance between probe targets

As described in Sect. 2.3, the hand-held probe is equipped with two targets – i.e., $A \equiv (X_A, Y_A, Z_A)$ and $B \equiv (X_B, Y_B, Z_B)$. The distance between the two probe devices (d_{AB}) is *a priori* known (see Figure 5-b). On the other hand, having localized the two targets, their Euclidean distance can be estimated as:

$$\tilde{d}_{AB} = \|A - B\| = \sqrt{(X_A - X_B)^2 + (Y_A - Y_B)^2 + (Z_A - Z_B)^2} \ . \tag{19}$$

The residual ε_{AB} is defined as:

$$\varepsilon_{AB} = \tilde{d}_{AB} - d_{AB} \, . \tag{20}$$

In the absence of spatial/directional effects, it is reasonable to associate the ε_{AB} values to a zero-mean normal distribution (this hypothesis will also be tested empirically):

$$\varepsilon_{AB} \sim N(\mu_{AB} \approx 0, \sigma_{AB}) . \tag{21}$$

Assuming α as a type-I error, a further statistical test can be performed in order to evaluate measurement reliability. Let Q_{MIN} and Q_{MAX} be respectively the (α/2)-quantile and (1–α/2)-quantile of a normal distribution with mean μ_{AB} = 0 and standard deviation σ_{AB}.

For a given value of α, Q_{MIN} and Q_{MAX} can be expressed as multiples of the standard deviation σ_{AB}:

$$\begin{aligned} Q_{MIN} &= z_{\alpha/2} \cdot \sigma_{AB} \\ Q_{MAX} &= z_{1-\alpha/2} \cdot \sigma_{AB} \end{aligned} , \tag{22}$$

where $z_{\alpha/2}$ and $z_{(1-\alpha/2)}$ are the α/2- and (1–α/2)-quantiles of the standard normal distribution.

Again, the σ_{AB} value can be *a priori* estimated, during the preliminary stage of the system installation and calibration.

Every time a measurement is performed, MScMS-II diagnostics calculates the quantity in Eq. 20. [Q_{MIN}, Q_{MAX}] is assumed as the symmetrical acceptance interval for the measurement reliability test; i.e., if the calculated residual ε_{AB} satisfies the condition:

$$\varepsilon_{AB} \in [Q_{MIN}, Q_{MAX}] , \tag{23}$$

the measurement can be considered reliable, hence it is accepted.

3.2.1 Set up of test parameters

As usual, the risk level α is established by the user.
Similarly to the previous diagnostic test (in Sect. 3.1), the standard deviation σ_{AB} can be evaluated empirically, on the basis of a reasonable number of angular measurements.
A set of *M* points randomly distributed in the measurement space $\xi \subseteq \Re^3$ are measured according to a random sequence. For each *j*-th measurement (where *j* = 1…*M*), a residual $\varepsilon_{AB,j}$ is calculated.
In absence of systematic error causes and time or spatial/directional effects, we hypothesize the same normal distribution for all the random variables $\varepsilon_{AB,j}$, i.e., $\varepsilon_{AB,j} \sim N(\mu_{AB}, \sigma_{AB})$,
being $\hat{\mu}_{AB} = \left(\sum_{j=1}^{M} \varepsilon_{AB,j} \right) \Big/ M \approx 0$ (to be tested).
The standard deviation may be estimated as:

$$\hat{\sigma}_{AB} = \sqrt{\left[\sum_{j=1}^{M} \left(\varepsilon_{AB,j} - \hat{\mu}_{AB} \right)^2 \right] \Big/ (M-1)} \,. \tag{24}$$

The resulting value of $\hat{\sigma}_{AB}$ is considered as the reference value for the test. Test limits defined in Eq. 22 become:

$$\begin{aligned} Q_{MIN} &= z_{\alpha/2} \cdot \hat{\sigma}_{AB} \\ Q_{MAX} &= z_{1-\alpha/2} \cdot \hat{\sigma}_{AB} \end{aligned} \,. \tag{25}$$

3.2.2 Experimental example

In order to estimate σ_{AB}, the following steps were followed:

- A sample of *M* = 601 points, randomly measured by the hand-held probe, was considered.
- The coordinates of each probe target were evaluated by solving the triangulation problem seen in Sect. 2.2, and d_{AB} is estimated according to Eq. 19. A sample of 601 residuals ($\varepsilon_{AB,j}$, *j* = 1…*M*) was obtained.
- The zero-mean normal distribution of residuals was verified by the Anderson-Darling normality test at p<0.05.
- The standard deviation σ_{AB} was estimated using Eq. 24. The result is $\hat{\sigma}_{AB} = 0.82\,\text{mm}$ (see Table 4 for details).

Having assumed α = 5%, the resulting (1–α) = 95% confidence interval for ε_{AB} is [$z_{\alpha/2} \cdot \sigma_{AB}$, $z_{1-\alpha/2} \cdot \sigma_{AB}$] = [-1.96·0.82, 1.96·0.82] = [-1.61, 1.61] mm. A generic measured point can not be considered unreliable if $\left\|\varepsilon_{AB}\right\| \le z_{1-\alpha/2} \cdot \sigma_{AB} = 1.61\,\text{mm}$.

Now, considering a measurement similar to that exemplified in Section 3.1.2, let suppose that probe target *A* is placed on point *P*. Due to the false-target effect, the localization algorithm produces an incorrect localization of target $A \equiv (90.1, 1026.5, 308.8)$.

Target *B*'s localization, which is not affected by the false-target error, results in $B \equiv (283.3, 1037.3, 300.1)$.

The residual concerning the *a priori* known distance *AB* is $\varepsilon_{AB} = -6.29$ mm. This value is not included in the acceptance interval [-1.61; 1.61] mm, hence the system diagnostics automatically suggests to reject the measurement.

Sample size: *M*	601
Mean estimate: $\hat{\mu}_{AB} = \left(\sum_{j=1}^{M} \varepsilon_{AB,j}\right) \Big/ M$	0.97 mm
Standard deviation estimate: $\hat{\sigma}_{AB} = \sqrt{\left(\sum_{j=1}^{M} \varepsilon_{AB,j}^{\,2}\right) \Big/ (M-1)}$	0.82 mm
Maximum: $\varepsilon_{AB_{MAX}} = Max\{\varepsilon_{AB,j} \mid j = 1...M\}$	2.60 mm
Minimum: $\varepsilon_{AB_{MIN}} = Min\{\varepsilon_{AB,j} \mid j = 1...M\}$	-2.42 mm

Table 4. Detailed data concerning the estimation of σ_{AB}.

After the obstacle is removed, the new coordinates of *A* become $A \equiv (83.3, 1036.3, 299.6)$. The new residual is $\varepsilon_{AB} = 2.9 \cdot 10^{-2}$ mm, therefore the new localization is accepted.

3.3 Test 3: Local test for identifying purportedly faulty device(s)

If at least one of the global tests fails, a local test needs to be performed for failure isolation. The philosophy is to correct the results of a dubious measurement, by excluding the network device(s) that purportedly caused the fault, without losing the observations from the remaining network devices. In this way, the target localization process is never interrupted, even in the presence of local anomalies.

Referring to the measurements carried out by each network device, the two types of residuals defined in Sect. 3.1 can be standardized as:

$$\frac{\varepsilon_{\theta i}}{\sigma_\theta} \text{ and } \frac{\varepsilon_{\varphi i}}{\sigma_\varphi} \qquad i = 1...N\,, \tag{26}$$

where:

σ_θ and σ_φ denote the standard deviations of the residuals related to the θ_i and φ_i angles respectively;

N denotes the number of network devices involved in the i-th measurement.

The standardised residuals can be used for outlier detection with uncorrelated and normally distributed observations in a sense that, if the i-th observation is not an outlier, then $\varepsilon_{\theta_i}/\sigma_\theta$ and $\varepsilon_{\varphi i}/\sigma_\varphi$ are normally distributed ~ $N(0,1)$. Each standardised residual is compared to a $\alpha/2$-quantile and a (1 – $\alpha/2$)-quantile of the standard normal distribution (i.e., $z_{\alpha/2}$ and $z_{1-\alpha/2}$), with the significance level α. The null-hypothesis, which denotes that the i-th observation is not an outlier, is rejected if at least one of the two standardised residuals in Eq. 26 is not included in the [$z_{\alpha/2}$, $z_{1-\alpha/2}$] symmetrical confidence interval, or its absolute value ≤ $z_{1-\alpha/2}$. An outlier in one standardized residual generally causes ones other residuals to be increased in absolute values.

Local testing is easy under the assumption that there is only one purportedly faulty device (or outlier) in the current measurement: the local angular observation with the largest (absolute value of the) standardised residuals, provided that it is beyond the confidence interval, is regarded as an outlier and the corresponding network device (D_i) is excluded from the triangulation problem.

The assumption that there is only one outlier is a severe restriction in the case measurements from more than one network device are degraded. However, the procedure can be extended to multiple outliers iteratively: after exclusion of a potentially faulty device, the statistical test and the rejection of one other device can be repeated for that epoch until no more outliers are identified [13]. Of course, assessment for such multiple outliers may give rise to extensive computations. However, they represent a very rare event.

3.3.1 Set up of test parameters

The parameters σ_θ and σ_φ in Eq. 26 are the same used in the (global) Test 1; therefore (see Sect. 3.1.1).

3.3.2 Application example

Returning to the example presented in Sect. 3.1.2 (in which device D_4 detects a false target), the relevant normalized residuals are reported in Table 5(a).

In this calculation we used the $\hat{\sigma}_\theta$ and $\hat{\sigma}_\varphi$ values previously estimated.

Network device	Standardized residuals (a)	(b)
D_1	$\varepsilon_{\theta_1}/\hat{\sigma}_\theta = -0.59$ and $\varepsilon_{\varphi_1}/\hat{\sigma}_\varphi = 3.11$	$\varepsilon_{\theta_1}/\hat{\sigma}_\theta = -0.51$ and $\varepsilon_{\varphi_1}/\hat{\sigma}_\varphi = 1.94$
D_2	$\varepsilon_{\theta_2}/\hat{\sigma}_\theta = -0.69$ and $\varepsilon_{\varphi_2}/\hat{\sigma}_\varphi = 0.56$	$\varepsilon_{\theta_2}/\hat{\sigma}_\theta = -0.35$ and $\varepsilon_{\varphi_2}/\hat{\sigma}_\varphi = -0.01$
D_3	$\varepsilon_{\theta_3}/\hat{\sigma}_\theta = -0.10$ and $\varepsilon_{\varphi_3}/\hat{\sigma}_\varphi = 1.55$	$\varepsilon_{\theta_3}/\hat{\sigma}_\theta = 0.22$ and $\varepsilon_{\varphi_3}/\hat{\sigma}_\varphi = 0.82$
D_4	$\varepsilon_{\theta_4}/\hat{\sigma}_\theta = 7.26$ and $\varepsilon_{\varphi_4}/\hat{\sigma}_\varphi = -6.16$	(excluded)
D_5	$\varepsilon_{\theta_5}/\hat{\sigma}_\theta = -0.79$ and $\varepsilon_{\varphi_5}/\hat{\sigma}_\varphi = -0.53$	$\varepsilon_{\theta_5}/\hat{\sigma}_\theta = -0.27$ and $\varepsilon_{\varphi_5}/\hat{\sigma}_\varphi = 0.04$
D_6	$\varepsilon_{\theta_6}/\hat{\sigma}_\theta = 0.96$ and $\varepsilon_{\varphi_6}/\hat{\sigma}_\varphi = -1.53$	$\varepsilon_{\theta_6}/\hat{\sigma}_\theta = -0.88$ and $\varepsilon_{\varphi_6}/\hat{\sigma}_\varphi = -0.45$

Table 5. Standardized residuals for the measurement exemplified in Sect. 3.1.2: (a) before and (b) after the exclusion of the observations from D4.

Assuming α = 5%, the confidence interval is [$z_{\alpha/2}$ = -1.96, $z_{1-\alpha/2}$ = 1.96]. More than one residual is outside this interval – i.e., both the residuals of D_4 and one of D_1 – but the "prime suspect" is D_4, being the device with the highest (absolute) values of residuals. D_4 is then excluded and, repeating the localization, the new output is (83.2, 1036.5, 299.5) [mm]. All the standardized residuals are now contained within the confidence interval (see Table 5(b)).
Not surprisingly, the Test 1 – performed using only the observations from the five remaining devices – is satisfied; precisely, $EF(P) = 2.20 \leq \frac{\chi^2_{\nu=10,1-\alpha=0.95}}{5} \cong 3.66$.

4. IMPLICATIONS, LIMITATIONS AND FUTURE RESEARCH

The on-line diagnostics presented in the paper make it possible to monitor measurement reliability in real time, on the basis of some statistical tests. Although tests were implemented on MScMS-II, they are deliberately general and can be applied to any distributed LSDM system based on triangulation (e.g., iGPS, HiBall, etc.).
An important characteristic of these tests is their ability to selectively exclude faulty network device(s), without interrupting the measurement process.
In addition to these tests, we remark that MScMS-II implements other tests, specifically related to photogrammetric technology (e.g., tests concerning epipolar geometry), which were deliberately ignored in this paper [18].
The tests described in the paper require the estimation of some parameters; primarily the standard deviations related to the measurement residuals. These parameters can be evaluated empirically by performing some preliminary measurements under controlled conditions, according to the reasonable assumption of absence of time or spatial/directional effects. This operation can be performed during the system set-up and calibration, with no additional effort [19].

Since the on-line implementation of these tests requires a certain computational capacity, it could slow down the measurement process. However, this consequence is minimized due to (i) the high capacity of existing processors and (ii) test segmentation (i.e., local Test 3 is performed only after at least one of the global Tests 1 and 2 has detected the presence of potential anomalies). Also, a reduction of the computational workload can be achieved by linearizing the *EF*.
Finally, we remark that in (global) Test 2, it was considered a hand-held probe with two targets. However, it may be extended to probes with multiple targets (i.e., the so-called 6-DOF probes): in this case there would be multiple *a priori* known distances [7].
Future development of this research will be aimed at developing other diagnostic models for dynamic measurements (e.g., mobile object tracking). One possibility may be the integration of the models presented in this paper with techniques based on the Kalman filtering [20].

5. REFERENCES

[1] Franceschini, F., Galetto, M., Maisano, D., Mastrogiacomo, L., Pralio, B. (2011) Distributed Large-Scale Dimensional Metrology, Springer, London.

[2] Estler, W.T., Edmundson, K.L., Peggs, G.N., Parker, D.H. (2002) Large-scale metrology—an update. CIRP Ann. Manuf. Technol., 51:587-609.

[3] Peggs, G.N., Maropoulos, P.G., Hughes, E.B., Forbes, A.B., Robson, S., Ziebart, M., Muralikrishnan, B. (2009) Recent developments in large-scale dimensional metrology. Proceedings of the Institution of Mechanical Engineers, Part B: Journal of Engineering Manufacture, 223(6):571-595.

[4] Puttock, M. J. (1978) “Large-Scale Metrology”. Ann. CIRP, 21(1):351-356.

[5] Cuypers, W., Van Gestel, N., Voet, A., Kruth, J.P, Mingneau, J., Bleys, P. (2009) Optical measurement techniques for mobile and large-scale dimensional metrology. Optics and Lasers in Engineering, 47(3-4):292-300.

[6] Maisano, D., Jamshidi, J., Franceschini, F., Maropoulos, P.G., Mastrogiacomo, L., Mileham, A.R., Owen, G.W. (2008) Indoor GPS: system functionality and initial performance evaluation. International Journal of Manufacturing Research, 3(3):335-349.

[7] NPL (2013) http://www.npl.co.uk/news/npl-launches-portable-co-ordinate-measurement-systems-training-to-meet-industry-demands.

[8] Welch, G., Bishop, G., Vicci, L., Brumback, S., Keller, K. (2001) High-performance widearea optical tracking the hiball tracking system. Presence: Teleoperators and Virtual Environments, 10(1):1-21.

[9] Galetto, M., Mastrogiacomo, L., Pralio, B. (2011) MScMS-II: an innovative IR-based indoor coordinate measuring system for large-scale metrology applications. International Journal of Advanced Manufacturing Technology, 52(1-4):291-302.

[10] Lee, M.C., Ferreira, P.M. (2002) Auto-triangulation and auto-trilateration. Part 1. Fundamentals. Precision Engineering, 26(3):237-49.
[11] JCGM 200:2008 (2008) VIM—International vocabulary of metrology—basic and general concepts and associated terms (VIM). International Organization for Standardization, Geneva, Switzerland.
[12] Gertler, J.J. (1998) Fault detection and diagnosis in engineering system. Marcel Dekker, NewYork.
[13] Wieser, A., Petovello, M., Lachapelle, G. (2004) Failure Scenarios to be Considered with Kinematic High Precision Relative GNSS Positioning. Proc ION GNSS 2004, September 21-24. Long Beach, California, 1448-1459.
[14] Franceschini, F., Galetto, M., Maisano, D.A., Mastrogiacomo, L. (2009) On-line diagnostics in the Mobile Spatial coordinate Measuring System (MScMS). Precision Engineering, 33(4):408-417.
[15] Hartley, R., Zisserman, A. (2003) Multiple view geometry in computer vision. Cambridge University, 2nd edition, Cambridge (UK).
[16] Wolberg, J. (2005) Data Analysis Using the Method of Least Squares: Extracting the Most Information from Experiments. Springer. ISBN 3-540-25674-1.
[17] Box, G.E.P., Hunter, W.G., and Hunter, J.S. (1978). Statistics for experimenters. Wiley, New York.
[18] Luhmann, T., Robson, S., Kyle, S., Harley I. (2006). Close Range Photogrammetry Principles, Methods and Applications, Whittles, Scotland.
[19] Bar-Shalom, Y., Li, X.R., Kirubarajan, T. (2001) Estimation with applications to tracking and navigation. Wiley, New York.
[20] Galetto, M., Mastrogiacomo, L. (2013). Corrective algorithms for measurement improvement in MScMS-II (Mobile Spatial coordinate Measurement System). Precision Engineering, 37(1):228-234.